MIT JOINT PROGRAM
SCIENCE POLICY
GLOBAL CHANGE

Reprint 2017-16

Role of atmospheric oxidation in recent methane growth

M. Rigby, S.A. Montzka, R.G. Prinn, J.W.C. White, D. Young, S. O'Doherty, M. Lunt, A.L. Ganesan, A. Manning, P. Simmonds, P.K. Salameh, C.M. Harth, J. Mühle, R.F. Weiss, P.J. Fraser, L.P. Steele, P.B. Krummel, A. McCulloch and S. Park

Reprinted with permission from *PNAS*, 114(21): 5373–5377.

The **MIT Joint Program on the Science and Policy of Global Change** combines cutting-edge scientific research with independent policy analysis to provide a solid foundation for the public and private decisions needed to mitigate and adapt to unavoidable global environmental changes. Being data-driven, the Joint Program uses extensive Earth system and economic data and models to produce quantitative analysis and predictions of the risks of climate change and the challenges of limiting human influence on the environment—essential knowledge for the international dialogue toward a global response to climate change.

To this end, the Joint Program brings together an interdisciplinary group from two established MIT research centers: the **Center for Global Change Science (CGCS)** and the **Center for Energy and Environmental Policy Research (CEEPR)**. These two centers—along with collaborators from the Marine Biology Laboratory (MBL) at Woods Hole and short- and long-term visitors—provide the united vision needed to solve global challenges.

At the heart of much of the program's work lies MIT's Integrated Global System Model. Through this integrated model, the program seeks to discover new interactions among natural and human climate system components; objectively assess uncertainty in economic and climate projections; critically and quantitatively analyze environmental management and policy proposals; understand complex connections among the many forces that will shape our future; and improve methods to model, monitor and verify greenhouse gas emissions and climatic impacts.

This reprint is intended to communicate research results and improve public understanding of global environment and energy challenges, thereby contributing to informed debate about climate change and the economic and social implications of policy alternatives.

—Ronald G. Prinn and John M. Reilly,
Joint Program Co-Directors

MIT Joint Program on the Science and Policy of Global Change

Massachusetts Institute of Technology
77 Massachusetts Ave., E19-411
Cambridge MA 02139-4307 (USA)

T (617) 253-7492 **F** (617) 253-9845
globalchange@mit.edu
http://globalchange.mit.edu

SEE COMMENTARY

Role of atmospheric oxidation in recent methane growth

Matthew Rigby[a,1], Stephen A. Montzka[b], Ronald G. Prinn[c], James W. C. White[d], Dickon Young[a], Simon O'Doherty[a], Mark F. Lunt[a], Anita L. Ganesan[e], Alistair J. Manning[f], Peter G. Simmonds[a], Peter K. Salameh[g], Christina M. Harth[g], Jens Mühle[g], Ray F. Weiss[g], Paul J. Fraser[h], L. Paul Steele[h], Paul B. Krummel[h], Archie McCulloch[a], and Sunyoung Park[i]

[a]School of Chemistry, University of Bristol, Bristol BS8 1TS, United Kingdom; [b]Earth System Research Laboratory, National Oceanic and Atmospheric Administration, Boulder, CO 80305; [c]Center for Global Change Science, Massachusetts Institute of Technology, Cambridge, MA 02139; [d]Institute of Arctic and Alpine Research, University of Colorado, Boulder, CO 80309; [e]School of Geographical Sciences, University of Bristol, Bristol BS8 1SS, United Kingdom; [f]Hadley Centre, Met Office, Exeter EX1 3PB, United Kingdom; [g]Scripps Institution of Oceanography, University of California, San Diego, La Jolla, CA 92093; [h]Climate Science Centre, Commonwealth Scientific and Industrial Research Organization Oceans and Atmosphere, Aspendale, VIC 3195, Australia; and [i]Department of Oceanography, Kyungpook National University, Daegu 41566, Republic of Korea

Edited by Mark H. Thiemens, University of California, San Diego, La Jolla, CA, and approved March 16, 2017 (received for review October 3, 2016)

The growth in global methane (CH_4) concentration, which had been ongoing since the industrial revolution, stalled around the year 2000 before resuming globally in 2007. We evaluate the role of the hydroxyl radical (OH), the major CH_4 sink, in the recent CH_4 growth. We also examine the influence of systematic uncertainties in OH concentrations on CH_4 emissions inferred from atmospheric observations. We use observations of 1,1,1-trichloroethane (CH_3CCl_3), which is lost primarily through reaction with OH, to estimate OH levels as well as CH_3CCl_3 emissions, which have uncertainty that previously limited the accuracy of OH estimates. We find a 64–70% probability that a decline in OH has contributed to the post-2007 methane rise. Our median solution suggests that CH_4 emissions increased relatively steadily during the late 1990s and early 2000s, after which growth was more modest. This solution obviates the need for a sudden statistically significant change in total CH_4 emissions around the year 2007 to explain the atmospheric observations and can explain some of the decline in the atmospheric $^{13}CH_4/^{12}CH_4$ ratio and the recent growth in C_2H_6. Our approach indicates that significant OH-related uncertainties in the CH_4 budget remain, and we find that it is not possible to implicate, with a high degree of confidence, rapid global CH_4 emissions changes as the primary driver of recent trends when our inferred OH trends and these uncertainties are considered.

methane | hydroxyl | inversion | methyl chloroform | 1,1,1-trichloroethane

Methane (CH_4), the second most important partially anthropogenic greenhouse gas, is observed to vary markedly in its year to year growth rate (Fig. 1). The causes of these variations have been the subject of much controversy and uncertainty, primarily because there is a wide range of poorly quantified sources and because its sinks are ill-constrained (1). Of particular recent interest are the cause of the "pause" in CH_4 growth between 1999 and 2007 and the renewed growth from 2007 onward (2–7). It is important that we understand these changes if we are to better project future CH_4 changes and effectively mitigate enhanced radiative forcing caused by anthropogenic methane emissions.

The major sources of CH_4 include wetlands (natural and agricultural), fossil fuel extraction and distribution, enteric fermentation in ruminant animals, and solid and liquid waste. Our understanding of the sources of CH_4 comes from two approaches: "bottom up," in which inventories or process models are used to predict fluxes, or "top down," in which fluxes are inferred from observations assimilated into atmospheric chemical transport models. Bottom-up methods suffer from uncertainties and potential biases in the available activity data or emissions factors or the extrapolation to large scales of a relatively small number of observations. Furthermore, there is no constraint on the global total emissions from bottom-up techniques. The top-down approach is limited by incomplete or imperfect observations and our understanding of atmospheric transport and chemical sinks. For CH_4, these difficulties result in a significant mismatch between the two methods (1).

The primary CH_4 sink is the hydroxyl radical (OH) in the troposphere, although smaller sinks also exist, such as methanotrophic bacteria in soils, oxidation by chlorine radicals in the marine boundary layer, and photochemical destruction in the stratosphere. Predictions of the magnitude and variability of OH in the current generation of atmospheric models have been shown to be diverse (8). Furthermore, because of its short lifetime, it is difficult to infer global OH concentrations using direct observations. Therefore, indirect observational methods are needed. The most commonly used approach has been to infer global OH concentrations from observed trends in 1,1,1-trichloroethane (CH_3CCl_3), whose primary sink is also reaction with OH in the troposphere (9–13). Recent work using this approach indicated that OH changes could have played a role in the pause in CH_4 that occurred after 1998 (3, 14).

Previous studies have shown that OH trends inferred using CH_3CCl_3 could be highly sensitive to systematic errors in the assumed emissions trends, particularly in the 1980s and early 1990s when emissions were changing rapidly (15). Some authors have attempted to reduce this source of uncertainty by including

Significance

Methane, the second most important greenhouse gas, has varied markedly in its atmospheric growth rate. The cause of these fluctuations remains poorly understood. Recent efforts to determine the drivers of the pause in growth in 1999 and renewed growth from 2007 onward have focused primarily on changes in sources alone. Here, we show that changes in the major methane sink, the hydroxyl radical, have likely played a substantial role in the global methane growth rate. This work has significant implications for our understanding of the methane budget, which is important if we are to better predict future changes in this potent greenhouse gas and effectively mitigate enhanced radiative forcing caused by anthropogenic emissions.

Author contributions: M.R., S.A.M., R.G.P., R.F.W., and P.J.F. designed research; M.R., M.F.L., and A.L.G. performed research; M.R., S.A.M., R.G.P., J.W.C.W., D.Y., S.O., M.F.L., A.L.G., A.J.M., P.G.S., P.K.S., C.M.H., J.M., R.F.W., P.J.F., L.P.S., P.B.K., A.M., and S.P. provided observations and analyzed data; and M.R., S.A.M., R.G.P., P.G.S., J.M., P.J.F., L.P.S., and A.M. wrote the paper.

The authors declare no conflict of interest.

This article is a PNAS Direct Submission.

See Commentary on page 5324.

[1]To whom correspondence should be addressed. Email: matt.rigby@bristol.ac.uk.

This article contains supporting information online at www.pnas.org/lookup/suppl/doi:10.1073/pnas.1616426114/-/DCSupplemental.

ENVIRONMENTAL SCIENCES

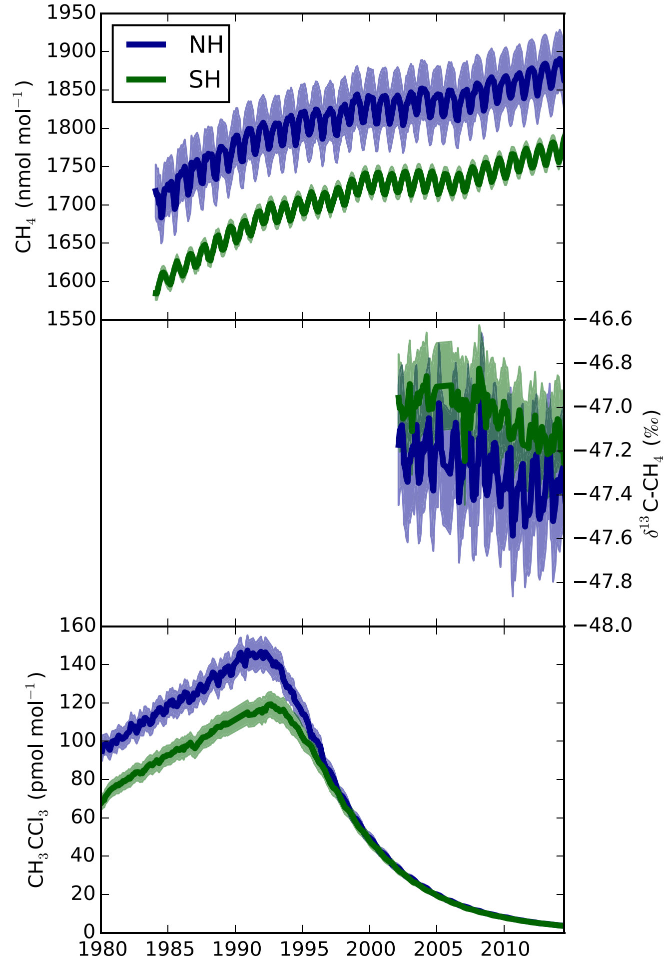

Fig. 1. (*Top*) NOAA observations of CH_4. (*Middle*) INSTAAR observations of δ^{13}C-CH_4. (*Bottom*) The AGAGE observations of CH_3CCl_3. Each plot shows the northern hemisphere (NH) and southern hemisphere (SH) means, and shading indicates the assumed 1-sigma model and measurement uncertainty as defined in *SI Materials and Methods*.

CH_3CCl_3 emissions as part of the inversion (12). However, these studies assumed that emissions uncertainties were Gaussian and uncorrelated between years, potentially reducing the impact of systematic errors in the a priori emissions model. Furthermore, with a few exceptions (16), most work has derived OH separately to CH_4 and its global $^{13}C/^{12}C$ source signature, limiting the propagation of uncertainty in OH through to the derived CH_4 fluxes. The inability to quantify CH_3CCl_3 systematic emissions uncertainties may be particularly problematic in recent years when, as a result of its production and consumption ban under the Montreal Protocol, reported consumption has dropped to very low levels, but evidence of continued emissions can still be seen in atmospheric observations (Fig. S1) (17, 18). Therefore, the assumptions that were used in early estimates of CH_3CCl_3 emissions, which were based on industry surveys at a time when CH_3CCl_3 was widely used (19), are unlikely to hold in recent decades.

In contrast to previous approaches, the method used in this paper explicitly includes a model of the CH_3CCl_3 emissions processes in the estimation scheme. Information regarding the global emissions of long-lived trace gases, such as CH_3CCl_3, can be derived simultaneously with their atmospheric sinks by jointly considering factors such as the long-term trend in concentration and the interhemispheric gradient (20). We extend this approach here by including the uncertain emissions and atmospheric model parameters jointly in a hierarchical Bayesian estimation framework that is informed by atmospheric data from multiple species. This method ensures that uncertainties in each component are propagated throughout the system. A full list of model parameters explored in the inversion is given in Table S1.

To focus on the uncertainties in the CH_3CCl_3 emissions model, we chose to use a computationally efficient "box model" of atmospheric transport and chemistry that included two tropospheric boxes and one stratospheric box. Previous authors have noted that the use of atmospheric box models with annually repeating transport can cause erroneous fluctuations in derived OH concentrations over periods of around 3 y or less, particularly during periods when emissions of CH_3CCl_3 were relatively large (15). However, recent studies have shown that, at least in recent years when atmospheric CH_3CCl_3 gradients are small, OH inversions based on box models agree very closely (to within ∼1%) with 3D model inversions using analyzed meteorology (13) or that OH variations derived using box models can be used to simulate realistic CH_3CCl_3 trends using 3D models (14). Therefore, in this paper, we primarily focus on longer-term OH trends, and we expect that our findings for recent decades would not be substantially different if a more complex model was used.

The atmospheric and emissions model parameters were constrained in a multispecies inversion using monthly mean observations of atmospheric CH_3CCl_3 from both the Advanced Global Atmospheric Gases Experiment (AGAGE) (21) and National Oceanic and Atmospheric Administration (NOAA) (4, 13) networks along with NOAA CH_4 data and ^{13}C-CH_4 observations from the University of Colorado's Institute of Arctic and Alpine Research (INSTAAR) (22, 23) (Fig. 1). Colocated AGAGE and NOAA observations were found to exhibit somewhat different long-term CH_3CCl_3 trends. Therefore, two sets of inversions were performed based on the CH_3CCl_3 observations from each network (Fig. S2). The AGAGE CH_4 observations were not used in the main part of this study, because they were found to agree very closely with NOAA data but cover a shorter time period. Additional details about the observations are provided in *SI Materials and Methods*, and the site locations are shown in Table S2.

Results

Rows 1 and 2 in Fig. 2 show the simultaneously derived OH concentrations and CH_3CCl_3 emissions inferred from independent application of our approach using the AGAGE or NOAA observations. A comparison between the observations and the model is shown in Fig. S3. The median solution shows a relatively small OH trend in the 1980s and 1990s [with smaller interannual variability than previous CH_3CCl_3 inversions (11, 12, 24)] followed by an upward trend in OH concentration on the order of 10% from the late 1990s to 2004 (11 ± 13 and $9 \pm 12\%$ increases for AGAGE and NOAA, respectively, between 1998 and 2004). This trend is of a similar size to those highlighted in previous studies using CH_3CCl_3 (14, 24). Post-2004, our median estimate shows a decline in OH. This finding would suggest that at least some fraction of the post-2007 CH_4 growth could be attributable to declining OH. By carrying out a set of linear regressions on the post-2007 OH estimates from our a posteriori ensemble of model states, we find a 70 or 64% probability that OH exhibited some level of negative trend during this period when AGAGE or NOAA data, respectively, were used (the mean differences between the 2004 and 2014 OH concentrations were $-8 \pm 11\%$ and $-11 \pm 11\%$, respectively). In addition to this trend are several features of our OH inversion that are important to note. First, significant uncertainties remain in the global OH concentration, such that it is possible to draw a "constant OH" line that is consistent with the observation-derived OH within its uncertainties. Second, small differences in the CH_3CCl_3 trend and

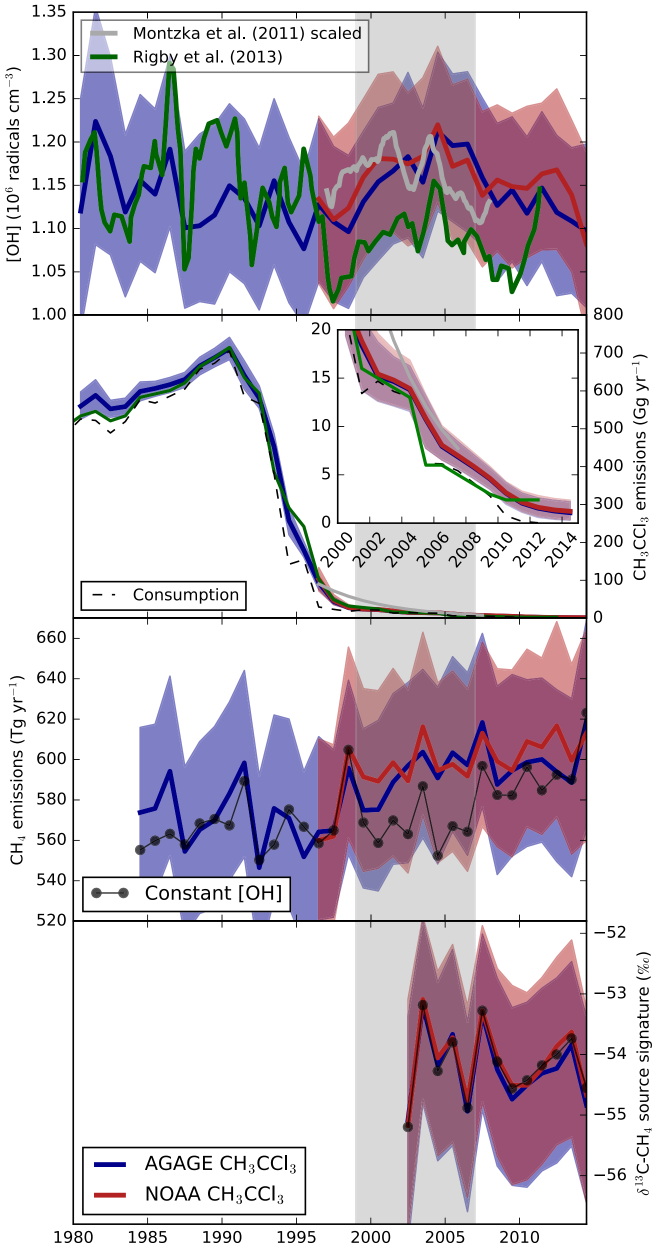

Fig. 2. (Row 1) Inferred tropospheric annual mean OH concentration. (Row 2) Global CH_3CCl_3 emissions. (Row 3) Global CH_4 emissions. (Row 4) Global $^{13}C/^{12}C$ source isotope ratio of CH_4. The blue lines and shading show quantities inferred when AGAGE CH_3CCl_3 data were used, and the red lines and shading show those inferred using NOAA CH_3CCl_3 data. Lines indicate the medians, and the shading shows the 16th to 84th percentiles ($\sim\pm1$ sigma). The green and gray lines in rows 1 and 2 show estimates from previous studies that used the same observations but different methodologies and emissions (13, 24). *Inset* in row 2 zooms in on the CH_3CCl_3 emissions from 2000 to 2014. The black lines in rows 3 and 4 show the methane and isotopologue changes inferred when interannually repeating OH was used. The gray shading shows the approximate start and end of the methane pause. Numerical values of the quantities in this figure are available in Dataset S1.

interhemispheric gradient measured by the two independent networks lead to variations in the derived OH concentration and CH_3CCl_3 emissions. However, these differences are small compared with the other uncertainties in the system.

Differences between our derived CH_3CCl_3 emissions and those assumed previously (Fig. 2, row 2) explain part of the discrepancy between our OH trends and those derived in previous studies (Fig. 2, row 1), although other factors, such as the treatment of the ocean sink, also contribute (*SI Materials and Methods*). Our global CH_3CCl_3 emissions estimates differ from the previous estimates shown in Fig. 2 in that they have been adjusted in the inversion to be consistent with atmospheric observations (and in particular, the interhemispheric CH_3CCl_3 mol fraction gradient) instead of being imposed based on bottom-up models or an assumed rate of decline (13, 24). The CH_3CCl_3 emissions derived in our inversion indicate that there was ongoing release of CH_3CCl_3 to the atmosphere, at least through 2014, despite national reports indicating that use of this substance ceased in 2013 (25). Analysis of high-frequency AGAGE data confirms that emissions persisted throughout this period upwind of some monitoring sites (Fig. S1).

In addition to our multispecies inversion, we carried out an inversion for OH concentrations and CH_3CCl_3 emissions using only CH_3CCl_3 observations (Fig. S4). We find that the OH concentrations and variability derived in this analysis lead to a similar result to the multispecies inversion, indicating that the constraint on OH is primarily from CH_3CCl_3 rather than CH_4 and its $^{13}C/^{12}C$ ratio. Therefore, the timing of the rise and fall in inferred OH has not been significantly influenced by "knowledge" of the pause and renewed growth in CH_4.

Our multispecies inversion allows us to propagate information on the derived OH concentration and its uncertainty through to estimates of CH_4 emissions. We find that, similar to OH concentration, it is possible to draw a "constant CH_4 emissions" line within the derived uncertainties (Fig. 2, row 3). However, the median solution suggests a relatively steady upward trend from the mid-1990s to the mid-2000s followed by a period of smaller growth. We note that our result does not require a sudden, statistically significant increase in CH_4 emissions in 2007, as suggested elsewhere, to explain the observations (5–7, 26, 27). Instead, it is implied that the rise in atmospheric mole fractions in 2007 is consistent with the decline in OH concentrations post-2004 overlaid on a gradual rise in CH_4 emissions with some additional interannual variability on the order of 10 Tg y^{-1}.

Row 3 in Fig. 2 also shows an inversion where OH is constrained to be interannually repeating. In this scenario, CH_4 emissions remain at a relatively low level throughout the 2000s compared with the varying OH inversions until around 2007, when they sharply increase. Compared with the 5-y period before 2007, emissions from 2007 to 2011 (inclusive) were 22 ± 9 Tg y^{-1} higher in this scenario [similar to other studies that had assumed constant OH (28)]. In contrast, for the inversions with the OH changes derived from AGAGE or NOAA CH_3CCl_3, this difference was found to be 4 ± 23 or 9 ± 22 Tg y^{-1}, respectively.

In our inversion, we determine the global $^{13}CH_4/^{12}CH_4$ source signature that would be required to match the observed atmospheric δ^{13}C-CH_4 (*SI Materials and Methods*) considering changes in OH and global CH_4 emissions (Fig. 2, row 4). The observations and modeling framework provide relatively weak constraints on this term, such that the uncertainties on annual $^{13}CH_4/^{12}CH_4$ source ratios are around an order of magnitude larger, at around 1‰, than the changes that would be required to match the observed trends, which are of the order of 0.1‰. Furthermore, we find that, because of the very long timescales over which methane isotopologues respond to source or sink perturbations (29), our derived source ratio values are significantly autocorrelated, meaning that, in our inversion, the derived annual values cannot be considered fully independent of one another (Fig. S5).

Discussion

We have presented an inversion that derives global OH concentrations simultaneously with CH_3CCl_3 and CH_4 emissions and the $^{13}CH_4/^{12}CH_4$ source ratio using atmospheric observations of CH_3CCl_3, CH_4, and δ^{13}C-CH_4. Our median solution shows that OH increased from the late 1990s to 2004 before declining until 2014, albeit with an uncertainty that is of similar magnitude to the change. The median solution suggests that OH changes have contributed to the recent pause and growth in CH_4 as reflected in the median CH_4 emissions, which only change slowly after the late 1990s. In contrast, our constant OH inversion shows a relatively sudden emissions increase in 2007. It is interesting to note that these two sets of derived emissions agree relatively well during the 1990s (at levels of ∼560 Tg y^{-1}) and after 2010 (∼600 Tg y^{-1}), but the trajectory of the transition is different, with most of the increase occurring in the late 1990s if OH is allowed to change but primarily around 2007 if it is not. However, it is also important to note that the median solution of the constant OH inversion falls within the 1-sigma range of the "varying OH" inversions.

Notwithstanding the uncertainties, our findings are in contrast to recent work in which a 3D model of atmospheric transport and chemistry predicted only a gradual decrease in methane lifetime over the last three decades and therefore, that emissions changes were primarily responsible for the CH_4 growth (7). We also provide an alternative perspective to another study that attributed much of the recent growth in CH_4 and δ^{13}C-CH_4 to tropical wetland emissions based partly on the finding that there was no clear signal of an OH change in other reduced chemical tracers (CH_3CCl_3 had not been considered) (6). Other authors have investigated and ruled out OH changes as being the sole driver of recent trends in studies that used δ^{13}C-CH_4 and ethane (C_2H_6) to assign the growth in methane to livestock and oil and gas extraction, respectively (5, 26).

Forward model simulations with our derived OH and a constant ^{13}C-CH_4 source show a decline in atmospheric δ^{13}C-CH_4 post-2006, showing that OH trends likely contributed to the recent δ^{13}C-CH_4 trends in our inversion (Fig. S6). Although the precise contribution of OH to the observed trend is difficult to isolate from other influences, it is likely that our derived changes are not sufficient to explain the entire recent decline in δ^{13}C-CH_4 and that some change in the source signature has also occurred as has been suggested previously (26). However, as described above, the uncertainties on the source signature in our inversion are much larger than the required change in source signature, making the precise identification of a change in one or more source sectors difficult.

Some recent studies have pointed to an "upturn" in global concentrations of ethane (C_2H_6), coincident with the recent rise in CH_4 (5, 30, 31), which may imply an increase in CH_4 emissions caused by an increase in oil and gas extraction. Column-averaged measurements in the background atmosphere reveal trends in C_2H_6 between 2007 and 2014 of 23 (95% confidence interval = 18, 28) and −4 (95% confidence interval = −6, −1) pmol mol^{-1} y^{-1} in the northern and southern hemispheres, respectively (5). Because C_2H_6 is primarily removed from the atmosphere via reaction with OH, we also expect changes in OH to have an impact on C_2H_6 concentrations, even if emissions have not changed. By running our model forward with constant C_2H_6 emissions [which were tuned to match the mean northern and southern hemispheric observed mole fractions (5)] (Fig. S7) and our derived OH concentrations, we find that it is possible to explain a global background C_2H_6 growth rate of 9 (95% confidence interval = −11, 30) and 3 (95% confidence interval = −4, 11) pmol mol^{-1} y^{-1} in the northern and southern hemispheres, respectively, from 2007 to 2014. The timing of transition from declining to growing C_2H_6 mol fractions in the northern hemisphere coincides within 1 or 2 y with change from growing to declining OH in our inversion (Fig. S7). Therefore, it is possible that some of the recent upturn in northern hemispheric C_2H_6 is also caused by changes in OH concentration. Our constant emissions simulation does not match the continued downward trend in southern hemispheric C_2H_6, although the uncertainties in our estimates overlap with the observed trend.

As we stress above, it is important to note the magnitude of the uncertainties in our inversions, which we believe are more comprehensive than previous work, because they incorporate several systematic factors, particularly relating to CH_3CCl_3 emissions. If OH changes and their uncertainty are not considered, a sudden and statistically significant increase in CH_4 emissions after 2006 is required to fit the observations. Although we cannot rule out this scenario, in our inversions in which the recent CH_3CCl_3 budget is objectively considered, a trajectory in which CH_4 emissions have changed more gradually during the late 2000s is also plausible. Our study highlights that without careful consideration of the CH_4 sink and its uncertainty, it would be possible to draw misleading conclusions regarding the emissions trend when long-term records of background atmospheric observations are used. Our median estimate suggests an important role for OH in the recent CH_4 pause and growth overlaid on a relatively gradual increase in CH_4 emissions over the last two decades.

Materials and Methods

Atmospheric mole fractions were simulated using a box model atmosphere, which accounted for mixing between the two tropospheric hemispheres, and exchange with the stratosphere. Loss of CH_3CCl_3 and CH_4 occurred primarily through reaction with OH in the model troposphere [with the potential for differences in the northern and southern OH concentrations (32)]. The model also included a first-order loss of each compound in the stratosphere (all stratospheric losses were considered to contribute to a single stratospheric loss rate), first-order sinks for CH_4 in the troposphere because of reaction with chlorine and uptake by methanotrophs in soils (1), and an ocean uptake for CH_3CCl_3 according to previous ocean model estimates (33). Isotopic fractionation of CH_4 was assumed to occur for each sink based on recent estimates (34–37). Emissions of CH_3CCl_3 were estimated using a model that took as an input consumption or use of CH_3CCl_3. Uncertain parameters in the atmospheric and emissions model were estimated in the inversion along with estimates of the annual hemispheric CH_4 surface flux and $^{13}CH_4/^{12}CH_4$ source signature and global annual OH concentration. By exploring some of the major unknown parameters in this multispecies framework, the influence of uncertainties in each parameter and the atmospheric data could be propagated through the system (Table S1 shows a list of model parameters). The AGAGE, NOAA, and INSTAAR data (Fig. 1) were used to constrain the model parameters using a hierarchical Bayesian framework, which was solved using a Markov Chain Monte Carlo (MCMC) algorithm (38). The MCMC approach iteratively explores model states, randomly accepting or rejecting proposed parameter values with a probability dependent on the ratio of posterior probability density of the "current" and proposed states. The outcome is a chain of parameter values that spans the posterior probability density functions. Atmospheric data from a subset of the three networks were used where predominantly "background" (unpolluted) air masses were sampled and time series of the order of a decade or more were available. The delta notation for observations of $^{13}C/^{12}C$ ratio in CH_4 is defined as

$$\delta = 1{,}000\left(\frac{R}{R_{std}} - 1\right), \quad [1]$$

where R is the $^{13}C/^{12}C$ ratio in CH_4, and R_{std} refers to a reference ratio (39); values are quoted in per mille (‰). Additional details are provided in *SI Materials and Methods*.

ACKNOWLEDGMENTS. We thank E. Dlugokencky for his continuing efforts to produce the NOAA CH_4 dataset and helpful comments on our manuscript. NOAA measurements of CH_4 and CH_3CCl_3 are supported, in part, by the NOAA Climate Program Office's AC4 Program and benefited from the technical assistance of C. Siso, B. Hall, G. Dutton, and J. Elkins. M.R. is supported by Natural Environment Research Council (NERC) Advanced Research Fellowship NE/I021365/1 and Natural Environment Research Council Grant NE/N016211/1. A.L.G. is supported by NERC Independent Research Fellowship NE/L010992/1. M.F.L. is supported by NERC Grants NE/I027282/1 and NE/M014851/1. The operations of the AGAGE instruments at Mace Head, Trinidad Head, Cape Matatula, Ragged Point, and Cape Grim are supported by NASA Grants NNX16AC98G [to Massachusetts Institute of Technology

(MIT)], NNX07AE89G (to MIT), NNX11AF17G (to MIT), NNX07AE87G [to Scripps Institution of Oceanography (SIO)], NNX07AF09G (to SIO), NNX11AF15G (to SIO), and NNX11AF16G (to SIO); Department of Energy and Climate Change Contract GA01081 to the University of Bristol; the Commonwealth Scientific and Industrial Research Organization, Australia; and the Bureau of Meteorology, Australia. Measurements from Gosan, Korea are supported by the Basic Science Research Program through the National Research Foundation of Korea (Grant NRF-2013R1A1A2057880).

1. Kirschke S, et al. (2013) Three decades of global methane sources and sinks. *Nat Geosci* 6:813–823.
2. Dlugokencky EJ, et al. (2003) Atmospheric methane levels off: Temporary pause or a new steady-state? *Geophys Res Lett* 30:3–6.
3. Rigby M, et al. (2008) Renewed growth of atmospheric methane. *Geophys Res Lett* 35:L22805.
4. Dlugokencky EJ, et al. (2009) Observational constraints on recent increases in the atmospheric CH_4 burden. *Geophys Res Lett* 36:L18803.
5. Hausmann P, Sussmann R, Smale D (2016) Contribution of oil and natural gas production to renewed increase in atmospheric methane (2007–2014): Top–down estimate from ethane and methane column observations. *Atmos Chem Phys* 16:3227–3244.
6. Nisbet EG, et al. (2016) Rising atmospheric methane: 2007-2014 growth and isotopic shift. *Global Biogeochem Cycles* 30:1356–1370.
7. Dalsøren SB, Isaksen ISA (2006) CTM study of changes in tropospheric hydroxyl distribution 1990–2001 and its impact on methane. *Geophys Res Lett* 33:L23811.
8. Voulgarakis A, et al. (2013) Analysis of present day and future OH and methane lifetime in the ACCMIP simulations. *Atmos Chem Phys* 13:2563–2587.
9. Lovelock JE (1977) Methyl chloroform in the troposphere as an indicator of OH radical abundance. *Nature* 267:32–32.
10. Prinn RG, et al. (2001) Evidence for substantial variations of atmospheric hydroxyl radicals in the past two decades. *Science* 292:1882–1888.
11. Prinn RG, et al. (2005) Evidence for variability of atmospheric hydroxyl radicals over the past quarter century. *Geophys Res Lett* 32:L07809.
12. Bousquet P, Hauglustaine DA, Peylin P, Carouge C, Ciais P (2005) Two decades of OH variability as inferred by an inversion of atmospheric transport and chemistry of methyl chloroform. *Atmos Chem Phys* 5:2635–2656.
13. Montzka SA, et al. (2011) Small interannual variability of global atmospheric hydroxyl. *Science* 331:67–69.
14. McNorton J, et al. (2016) Role of OH variability in the stalling of the global atmospheric CH_4 growth rate from 1999 to 2006. *Atmos Chem Phys* 16:7943–7956.
15. Krol M, Lelieveld J (2003) Can the variability in tropospheric OH be deduced from measurements of 1,1,1-trichloroethane (methyl chloroform)? *J Geophys Res* 108:4125.
16. Pison I, Bousquet P, Chevallier F, Szopa S, Hauglustaine D (2009) Multi-species inversion of CH_4, CO and H_2; emissions from surface measurements. *Atmos Chem Phys* 9:5281–5297.
17. Krol MC, et al. (2003) Continuing emissions of methyl chloroform from Europe. *Nature* 421:131–135.
18. Reimann S, et al. (2005) Low European methyl chloroform emissions inferred from long-term atmospheric measurements. *Nature* 433:506–508.
19. McCulloch A, Midgley PM (2001) The history of methyl chloroform emissions: 1951-2000. *Atmos Environ* 35:5311–5319.
20. Liang Q, et al. (2014) Constraining the carbon tetrachloride (CCl_4) budget using its global trend and inter-hemispheric gradient. *Geophys Res Lett* 41:5307–5315.
21. Prinn RG, et al. (2000) A history of chemically and radiatively important gases in air deduced from ALE/GAGE/AGAGE. *J Geophys Res* 105:17751–17792.
22. White J, Vaughn BH (2015) *University of Colorado, Institute of Arctic and Alpine Research (INSTAAR), Stable Isotopic Composition of Atmospheric Methane (13c) from the NOAA ESRL Carbon Cycle Cooperative Global Air Sampling Network, 1998-2014, Version: 2015-08-03*. Available at ftp://aftp.cmdl.noaa.gov/data/trace_gases/ch4c13/flask/. Accessed April 1, 2016.
23. Miller JB, Mack KA, Dissly R, White JWC, Dlugockenky EJ, Tans PP (2002) Development of analytical methods and measurements of $^{13}C/^{12}C$ in atmospheric CH_4 from the NOAA Climate Monitoring and Diagnostics Laboratory Global Air Sampling Network. *J Geophys Res* 107:11-1–11-15.
24. Rigby M, et al. (2013) Re-evaluation of the lifetimes of the major CFCs and CH_3CCl_3 using atmospheric trends. *Atmos Chem Phys* 13:2691–2702.
25. UNEP (2016) *UNEP Ozone Secretariat Data Centre*. Available at ozone.unep.org/en/data-reporting/data-centre. Accessed February 21, 2015.
26. Schaefer H, et al. (2016) A 21st-century shift from fossil-fuel to biogenic methane emissions indicated by $^{13}CH_4$. *Science* 352:80–84.
27. Turner AJ, et al. (2016) A large increase in U.S. methane emissions over the past decade inferred from satellite data and surface observations. *Geophys Res Lett* 43:2218–2224.
28. Bergamaschi P, et al. (2013) Atmospheric CH_4 in the first decade of the 21st century: Inverse modeling analysis using SCIAMACHY satellite retrievals and NOAA surface measurements. *J Geophys Res Atmos* 118:7350–7369.
29. Tans PP (1997) A note on isotopic ratios and the global atmospheric methane budget. *Global Biogeochem Cycles* 11:77.
30. Helmig D, et al. (2016) Reversal of global atmospheric ethane and propane trends largely due to US oil and natural gas production. *Nat Geosci* 9:490–495.
31. Franco B, et al. (2015) Retrieval of ethane from ground-based FTIR solar spectra using improved spectroscopy: Recent burden increase above Jungfraujoch. *J Quant Spectrosc Radiat Transf* 160:36–49.
32. Patra PK, et al. (2014) Observational evidence for interhemispheric hydroxyl-radical parity. *Nature* 513:219–223.
33. Wennberg PO, Peacock S, Randerson JT, Bleck R (2004) Recent changes in the air-sea gas exchange of methyl choloroform. *Geophys Res Lett* 31:L16112.
34. Brenninkmeijer CAM, Lowe DC, Manning MR, Sparks RJ, van Velthoven PFJ (1995) The 13c, 14c, and 18o isotopic composition of CO, CH_4, and CO_2 in the higher southern latitudes lower stratosphere. *J Geophys Res* 100:26163–26172.
35. Allan W, Struthers H, Lowe DC (2007) Methane carbon isotope effects caused by atomic chlorine in the marine boundary layer: Global model results compared with Southern Hemisphere measurements. *J Geophys Res* 112:D04306.
36. Saueressig G, et al. (2001) Carbon 13 and D kinetic isotope effects in the reactions of CH_4 with $O(^1D)$ and OH: New Laboratory measurements and their implications for the isotopic composition of stratospheric methane. *J Geophys Res* 106(D19):23127–23138.
37. Lassey KR, Etheridge DM, Lowe DC, Smith AM, Ferretti DF (2007) Centennial evolution of the atmospheric methane budget: What do the carbon isotopes tell us? *Atmos Chem Phys* 7:2119–2139.
38. Hastings WK (1970) Monte Carlo sampling methods using Markov chains and their applications. *Biometrika* 57:97–109.
39. Craig H (1957) Isotopic standards for carbon and oxygen and correction factors for massspectrometric analysis of carbon dioxide. *Geochim Cosmochim Acta* 12:133–149.
40. Dlugokencky EJ, Steele LP, Lang PM, Masarie KA (1994) The growth rate and distribution of atmospheric methane. *J Geophys Res* 99:17021–17043.
41. O'Doherty S, et al. (2001) In situ chloroform measurements at Advanced Global Atmospheric Gases Experiment atmospheric research stations from 1994 to 1998. *J Geophys Res* 106:20429–20444.
42. Miller BR, et al. (2008) Medusa: A sample preconcentration and GC/MS detector system for in situ measurements of atmospheric trace halocarbons, hydrocarbons, and sulfur compounds. *Anal Chem* 80:1536–1545.
43. Cunnold DM, et al. (2002) In situ measurements of atmospheric methane at GAGE/AGAGE sites during 1985–2000 and resulting source inferences. *J Geophys Res* 107:4225.
44. Stevens CM, Rust FE (1982) The carbon isotopic composition of atmospheric methane. *J Geophys Res* 87:4879.
45. Tyler SC (1986) Stable carbon isotope ratios in atmospheric methane and some of its sources. *J Geophys Res* 91:13232.
46. Lowe DC, Brenninkmeijer CAM, Tyler SC, Dlugkencky EJ (1991) Determination of the isotopic composition of atmospheric methane and its application in the Antarctic. *J Geophys Res* 96:15455.
47. Patra PK, et al. (2011) TransCom model simulations of CH_4 and related species: Linking transport, surface flux and chemical loss with CH_4 variability in the troposphere and lower stratosphere. *Atmos Chem Phys* 11:12813–12837.
48. Cunnold DM, et al. (1983) The atmospheric lifetime experiment 3. Lifetime methodology and application to three years of $CFCl_3$ data. *J Geophys Res* 88(C13):8379–8400.
49. Cunnold DM, et al. (1994) Global trends and annual releases of CCl_3F and CCl_2F_2 estimated from ALE/GAGE and other measurements from July 1978 to June 1991. *J Geophys Res* 99(D1):1107–1126.
50. Sander SP, et al. (2011) Chemical Kinetics and Photochemical Data for Use in Atmospheric Studies: Evaluation Number 17 (NASA Jet Propulsion Laboratory, Pasadena, CA), Tech Rep 17.
51. Spivakovsky CM, et al. (2000) Three-dimensional climatological distribution of tropospheric OH: Update andevaluation. *J Geophys Res* 105:8931–8980.
52. Morice CP, Kennedy JJ, Rayner NA, Jones PD (2012) Quantifying uncertainties in global and regional temperature change using an ensemble of observational estimates: The HadCRUT4 data set. *J Geophys Res Atmos* 117:D08101.
53. Chipperfield MP, et al. (2013) Model estimates of lifetimes. SPARC Report on the Lifetimes of Stratospheric Ozone-Depleting Substances, Their Replacements, and Related Species, eds Reimann S, Ko MKW, Newman PA, Strahan SE (WMO/ICSU/IOC World Climate Research Programme, Zurich), SPARC Rep No. 6, WCRP-15/2013, Chap 5.
54. Ganesan AL, et al. (2014) Characterization of uncertainties in atmospheric trace gas inversions using hierarchical Bayesian methods. *Atmos Chem Phys* 14:3855–3864.
55. Roberts GO, Gelman A, Gilks WR (1997) Weak convergence and optimal scaling of random walk Metropolis algorithms. *Ann Appl Probab* 7(1):110–120.
56. Engel A, et al. (2013) Inferred lifetimes from observed trace-gas distributions. SPARC Report on the Lifetimes of Stratospheric Ozone-Depleting Substances, Their Replacements, and Related Species, eds Reimann S, Ko MKW, Newman PA, Strahan SE (WMO/ICSU/IOC World Climate Research Programme, Zurich), SPARC Rep No. 6, WCRP-15/2013, Chap 4.
57. Whiticar M, Schaefer H (2007) Constraining past global tropospheric methane budgets with carbon and hydrogen isotope ratios in ice. *Philos Trans R Soc Lond A* 365:1793–1828.
58. Snover AK, Quay PD, Hao WM (2000) The D/H content of methane emitted from biomass burning. *Global Biogeochem Cycles* 14:11–24.
59. Rigby M, Manning AJ, Prinn RG (2012) The value of high-frequency, high-precision methane isotopologue measurements for source and sink estimation. *J Geophys Res* 117:1–14.
60. Levin I, et al. (2012) No inter-hemispheric $\delta^{13}CH_4$ trend observed. *Nature* 486:E3–E4.
61. Lassey KR, Lowe DC, Manning MR (2000) The trend in atmospheric methane $\delta^{13}C$ and implications for isotopic constraints on the global methane budget. *Global Biogeochem Cycles* 14:41–49.

Joint Program Reprint Series - Recent Articles

For limited quantities, Joint Program publications are available free of charge. Contact the Joint Program office to order.
Complete list: http://globalchange.mit.edu/publications

2017-16 Role of atmospheric oxidation in recent methane growth. Rigby, M., S.A. Montzka, R.G. Prinn, J.W.C. White, D. Young, S. O'Doherty, M. Lunt, A.L. Ganesan, A. Manning, P. Simmonds, P.K. Salameh, C.M. Harth, J. Mühle, R.F. Weiss, P.J. Fraser, L.P. Steele, P.B. Krummel, A. McCulloch and S. Park, *Proceedings of the National Academy of Sciences,* 114(21): 5373–5377 (2017)

2017-15 A revival of Indian summer monsoon rainfall since 2002. Jin, Q. and C. Wang , *Nature Climate Change,* 7: 587–594 (2017)

2017-14 A Review of and Perspectives on Global Change Modeling for Northern Eurasia. Monier, E., D. Kicklighter, A. Sokolov, Q. Zhuang, I. Sokolik, R. Lawford, M. Kappas, S. Paltsev and P. Groisman, *Environmental Research Letters*, 12(8): 083001 (2017)

2017-13 Is Current Irrigation Sustainable in the United States? An Integrated Assessment of Climate Change Impact on Water Resources and Irrigated Crop Yields. Blanc, É., J. Caron, C. Fant and E. Monier, *Earth's Future*, 5(8): 877–892 (2017)

2017-12 Assessing climate change impacts, benefits of mitigation, and uncertainties on major global forest regions under multiple socioeconomic and emissions scenarios. Kim, J.B., E. Monier, B. Sohngen, G.S. Pitts, R. Drapek, J. McFarland, S. Ohrel and J. Cole, *Environmental Research Letters*, 12(4): 045001 (2017)

2017-11 Climate model uncertainty in impact assessments for agriculture: A multi-ensemble case study on maize in sub-Saharan Africa. Dale, A., C. Fant, K. Strzepek, M. Lickley and S. Solomon, *Earth's Future* 5(3): 337–353 (2017)

2017-10 The Calibration and Performance of a Non-homothetic CDE Demand System for CGE Models. Chen, Y.-H.H., *Journal of Global Economic Analysis* 2(1): 166–214 (2017)

2017-9 Impact of Canopy Representations on Regional Modeling of Evapotranspiration using the WRF-ACASA Coupled Model. Xu, L., R.D. Pyles, K.T. Paw U, R.L. Snyder, E. Monier, M. Falk and S.H. Chen, *Agricultural and Forest Meteorology*, 247: 79–92 (2017)

2017-8 The economic viability of Gas-to-Liquids technology and the crude oil-natural gas price relationship. Ramberg, D.J., Y.-H.H. Chen, S. Paltsev and J.E. Parsons, *Energy Economics*, 63: 13–21 (2017)

2017-7 The Impact of Oil Prices on Bioenergy, Emissions and Land Use. Winchester, N. and K. Ledvina, *Energy Economics*, 65(2017): 219–227 (2017)

2017-6 The impact of coordinated policies on air pollution emissions from road transportation in China. Kishimoto, P.N., V.J. Karplus, M. Zhong, E. Saikawa, X. Zhang and X. Zhang, *Transportation Research Part D*, 54(2017): 30–49 (2017)

2017-5 Twenty-First-Century Changes in U.S. Regional Heavy Precipitation Frequency Based on Resolved Atmospheric Patterns. Gao, X., C.A. Schlosser, P.A. O'Gorman, E. Monier and D. Entekhabi, *Journal of Climate*, online first, doi: 10.1175/JCLI-D-16-0544.1 (2017)

2017-4 The CO_2 Content of Consumption Across U.S. Regions: A Multi-Regional Input-Output (MRIO) Approach. Caron, J., G.E. Metcalf and J. Reilly, *The Energy Journal*, 38(1): 1–22 (2017)

2017-3 Human Health and Economic Impacts of Ozone Reductions by Income Group. Saari, R.K., T.M. Thompson and N.E. Selin, *Environmental Science & Technology*, 51(4): 1953–1961 (2017)

2017-2 Biomass burning aerosols and the low-visibility events in Southeast Asia. Lee, H.-H., R.Z. Bar-Or and C. Wang, *Atmospheric Chemistry & Physics*, 17, 965–980 (2017)

2017-1 Statistical emulators of maize, rice, soybean and wheat yields from global gridded crop models. Blanc, É., *Agricultural and Forest Meteorology,* 236, 145–161 (2017)

2016-25 Reducing CO_2 from cars in the European Union. Paltsev, S., Y.-H.H. Chen, V. Karplus, P. Kishimoto, J. Reilly, A. Löschel, K. von Graevenitz and S. Koesler, *Transportation*, online first (doi:10.1007/s11116-016-9741-3) (2016)

2016-24 Radiative effects of interannually varying vs. interannually invariant aerosol emissions from fires. Grandey, B.S., H.-H. Lee and C. Wang, *Atmospheric Chemistry & Physics,* 16, 14495–14513 (2016)

2016-23 Splitting the South: China and India's Divergence in International Environmental Negotiations. Stokes, L.C., A. Giang and N.E. Selin, *Global Environmental Politics*, 16(4): 12–31 (2016)

2016-22 Teaching and Learning from Environmental Summits: COP 21 and Beyond. Selin, N.E., *Global Environmental Politics*, 16(3): 31–40 (2016)

2016-21 Southern Ocean warming delayed by circumpolar upwelling and equatorward transport. Armour, K.C., J. Marshall, J.R. Scott, A. Donohoe and E.R. Newsom, *Nature Geoscience* 9: 549–554 (2016)

2016-20 Hydrofluorocarbon (HFC) Emissions in China: An Inventory for 2005–2013 and Projections to 2050. Fang, X., G.J.M. Velders, A.R. Ravishankara, M.J. Molina, J. Hu and R.G. Prinn, *Environmental Science & Technology*, 50(4): 2027–2034 (2016)

2016-19 The Future of Natural Gas in China: Effects of Pricing Reform and Climate Policy. Zhang, D. and S. Paltsev, *Climate Change Economics*, 7(4): 1650012 (2016)

MIT Joint Program on the Science and Policy of Global Change

Massachusetts Institute of Technology
77 Massachusetts Ave., E19-411
Cambridge MA 02139-4307 (USA)

T (617) 253-7492 **F** (617) 253-9845
globalchange@mit.edu
http://globalchange.mit.edu